Characterization of the oligomeric proanthocyanidin crofelemer toward development of an integrated mathematical model for comparison of complex molecules

By

Peter A. Kleindl

Submitted to the graduate degree program in Bioengineering and the Graduate Faculty of the University of Kansas in partial fulfillment of the requirements for the degree of Master of Science.

_____

Chairperson: Dr. M. Laird Forrest

_____

Dr. C. Russell Middaugh

_____

Dr. Xinmai Yang

Date Defended: July 21st, 2016

The Thesis Committee for Peter A. Kleindl certifies that this is the approved

version of the following thesis:

Characterization of the oligomeric proanthocyanidin crofelemer toward development of an integrated mathematical model for comparison of complex molecules

_____

Chairperson: Dr. M. Laird Forrest

Date approved:

Abstract

Regulatory approval of follow-on biologics and other generic versions of complex pharmaceutics requires that a potential biosimilar (test) product demonstrates similarity to an innovator (reference) product through a stepwise, totality of the evidence approach. Although the best statistical approaches for assessing analytical similarity are still under debate, these investigations rely heavily upon comparability of a given pharmaceutical's critical quality attributes (CQAs) – physicochemical and biological properties that are most relevant to clinical safety and efficacy. Selection of proper CQAs from the large amounts of physical, chemical, and biological data needed for sufficient characterization of these kinds of pharmaceutics can be difficult due to their inherent complexity and heterogeneity. Crofelemer, a botanically sourced polymeric proanthocyanidin, exhibits significant variation in final drug product resulting from processing and purification of the raw material and the botanical nature of the crude source material. From a single lot of crofelemer, various physically and chemically degraded samples were produced in an effort to create artificial lots with varying "similarity" to the reference starting material. Physical, chemical, and biological variability of the original and artificial lots were investigated using a variety of spectroscopic, chromatographic, mass-spectrometry, and biological techniques. The entirety of the analytical data collected for each crofelemer lot was then utilized in a machine learning approach to identify individual and/or combinations of CQAs which can accurately identify and distinguish subtle variations between the complex drug product (crofelemer) and the artificial lots comprised of its adulterated forms.

Acknowledgements

I would first like to thank Dr. Laird Forrest for all he has done in helping me develop as a scientist, along with his guidance through the challenges that have occasionally accompanied exploration into new fields of scientific discovery. Thank you to and Dr. Xinmai Yang for agreeing to sit on my committee and for being so accommodating with your time. Your insights throughout the project and feedback with the defense are greatly appreciated. I would also like to thank all of the other faculty, post docs and students with whom I was able to collaborate with: Dr. David Volkin, Dr. Christian Schöeneich, Dr. Aaron Smalter Hall, Dr. Eric Deeds, Dr. Tom Tolbert, Dr. Sangeeta Joshi, Dr. Jian Xiong, Dr. Jae Hyun Kim, Dr. Asha Hewarathna, Dr. Olivier Mozziconacci, Dr. Justin Douglas, Dr. Yu Wang, Sarah Neuenswander, Maulik Nariya, Apurva More, Solomon Okbazghi, Harshit Khasa, Sanjeev Agarwal, Naoki Mori, Ishan Shah, Derek White, Khalid Al-Kinani, Shaofeng Duan, and Yangjie Wei. Thank you to Dr. Adam Fisher and the other FDA members who have provided their guidance and expertise on the project. Having the opportunity to collaborate with the FDA and been an exciting and interesting experience. I must also thank my friends and fellow research partners in the Forrest lab: Dr. Ti Zhang, Dr. Sanjeewa Senadheera, Dr. Chad Groer, Dr. Shuang Cai, Dr. Qiuhong Yang, Ryan Moulder, Abby Petrulis, Ninad Varkhede, Jordan Hunt, and Jay Jha. Lastly, I would like to thank my family for being so supportive in every aspect of my life. Your encouragement and aspirations for me are what drive me to be better.

Table of Contents

1. Introduction

Biological and polymeric pharmaceutics are inherently more physically and chemically complex than small molecules. The consistency of these complex pharmaceutics is highly dependent on factors such as manufacturing processes and source materials. Accurate and sufficient characterization of each batch is crucial for ensuring the quality and efficacy of these therapeutic agents. To streamline this characterization, critical quality attributes (CQAs) are identified during development, which provide the most pertinent information for ensuring batch consistency and clinical outcome. Critical quality attributes are product specific, and variations in these attributes must be identified and accurately distinguished from the inherent heterogeneity of these complex pharmaceutics. Selecting relevant CQAs remains a difficult, yet necessary, step in the development of biological and other complex pharmaceutics.

Crofelemer is a botanically sourced polymeric proanthocyanidin currently approved by the FDA for the treatment of noninfectious secretory diarrhea in HIV/AIDs patients taking anti-retroviral therapies. Crofelemer is isolated from the red latex sap of the South American tree *Croton lechleri*. Hence, there is the potential for significant drug product variation arising from processing and purification of the raw material and the botanical nature of the crude latex source, e.g. growth conditions and specimen biodiversity. Crofelemer is a random polymer of (+)-catechin, (+)-gallocatechin, (-)-epicatechin, and (-)-epigallocatechin units. Polymer chains contain 1 to 28 repeating units and a number average of 5 to 7.5 units (Figure 1).

In 2010, the FDA established an abbreviated licensure pathway for the approval of "highly similar" versions of currently approved biological drugs. While statistical methods for evaluating similarity are still under debate, these methods all attempt to evaluate analytical similarities between test and reference compound CQAs. Hence, a fast and reliable method of

identifying CQAs through interpretation of vast amounts of variable physical, chemical, and biological characterization data, across lots and within lots themselves, is a key step in demonstrating biosimilarity of complex pharmaceutics.

In this study, ^{1}H and quantitative ^{13}C NMR techniques along with a kinetic fluorescence assay monitoring chloride ion efflux of T84 cell monolayers will be used to help characterize and evaluate a range of subtly degraded forms of single lot of crofelemer. This data was used in combination with a variety of other analytical methods through a machine learning approach to identify CQAs capable of distinguishing between the majority of crofelemer samples tested.

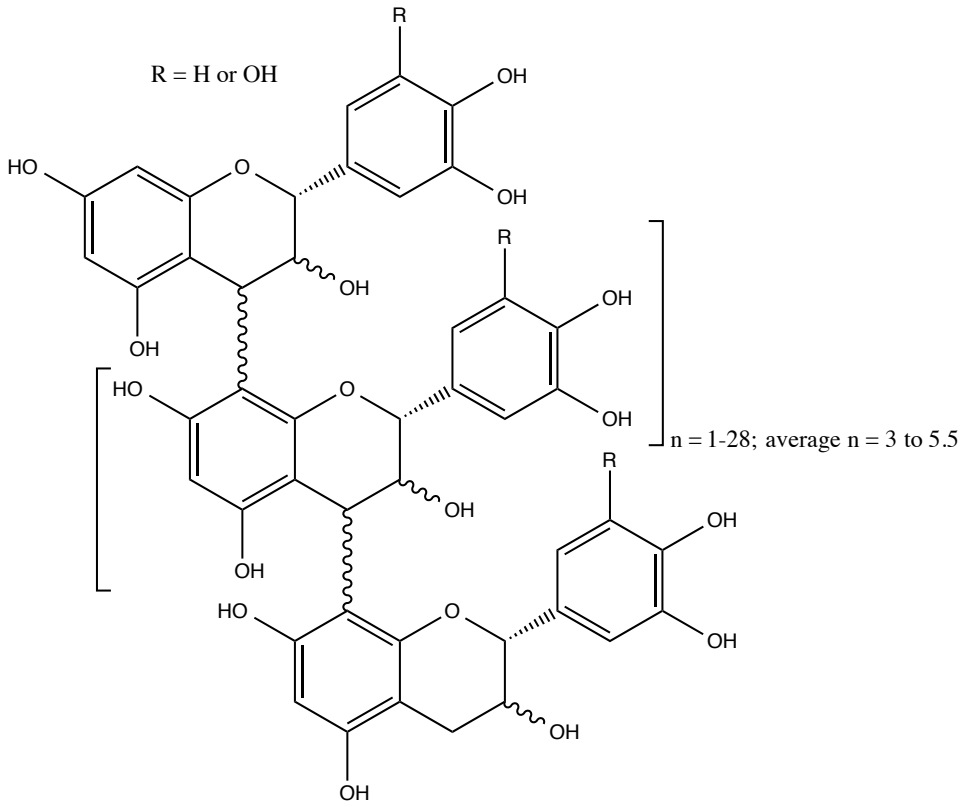

Figure 1: Structure of crofelemer outlined in the Fulyzaq® product label.

2. Background

2.1 Biotherapeutic Complexity and Similarity Assessment

The market for complex biotherapeutics has grown rapidly over the past few years into a multi-billion dollar industry, with 7 of the top 10 selling pharmaceuticals of 2014 being biologics (PMLiVE, 2016; Van Arnum, 2013). These impressive sales can most easily be contributed to their significantly larger costs compared to small molecule therapies, many in the order of several thousands of dollars per treatment. While extremely effective in their applications, the high price tags associated with treatment limit their practicality, and consequently their use, toward disease treatment. The inherent complexity of these molecules makes them difficult to produce, and often the consistency of a final product depends heavily on manufacturing process and source of origin. This heterogeneity must be well characterized, controlled, and documented when companies pursue regulatory approval. The time and expense associated with preliminary research, manufacturing, and regulatory approval translates into higher costs for patients taking theses types of drugs. Recently, various regulatory agencies (EMA, Japan, Canada, FDA) have established abbreviated regulatory guidelines for the approval of generic versions of these biological drugs, coined "biosimilars." By providing sufficient evidence of "similarity" between a potential biosimilar (test) product and a currently approved biological (reference) product, the competitor may be allowed to forgo extensive clinical investigations usually necessary for approval of innovator products. As patents begin to expire on brand name biological drugs, the market will open up for other companies to sell their own generic versions. The reduced capital costs for biosimilar approval and market competition will hopefully reduce the high costs currently associated with brand name biological drugs, increasing their application. However, there is still a need for a reliable, high(er) throughput means for determining "similarity"

between brand name biotherapeutics and a respective reference compounds. Streamlining this similarity determination will result in reduced time and cost toward approval, making biotherapeutics a more viable treatment option for patients.

2.2 Secretory Diarrhea and Chloride Ion Channels

Diarrhea continues to be a substantial contributor of morbidity and mortality worldwide("Diarrhoeal disease," April 2013). Diarrhea itself has various etiologies, and in many cases secretory mechanisms play a substantial role in disease severity. Secretory diarrhea occurs primarily through over-activation of chloride ion channels expressed by the epithelial cells that comprise the intestinal mucosa. These chloride channels help to regulate Cl- ion concentrations in the intestinal lumen, which together with Na+ helps regulate the osmotic gradient across the gut wall. The most common and well-understood perpetrators of secretory diarrhea are strains of *Vibrio cholerae* and *Escherichia coli* bacteria(Yeo, Crutchley, Cottreau, Tucker, & Garey, 2013). *V. cholerae* and *E. coli* secrete toxins (cholera toxin and E. coli heat-liable and heat-stable toxins, respectively) which initiate a signal cascade resulting in higher intracellular concentrations of cyclic adenosine monophosphate (cAMP) and subsequently increased Protein Kinase A (PKA) activity. PKA then phosphorylates the cystic fibrosis transmembrane conductance regulator (CFTR), initiating secretion of intracellular Cl- ions out of the cell and ultimately leading to accumulation of water in the luminal space.

There is growing evidence which suggests viral infections can initiate secretory and other forms of diarrhea(Lorrot & Vasseur, 2007). Rotavirus nonstructural protein (NSP4) is also classified as an enterotoxin, and has been shown to increase available intracellular concentrations of Ca^{2+} ions(Dong, Zeng, Ball, Estes, & Morris, 1997). Higher levels of intracellular Ca^{2+} can stimulate activation of

calcium activated chloride channels (CaCC), which are also responsible for Cl- ion efflux into the luminal space. The presence of transactivating factor protein (Tat), expressed during HIV-1 infection and replication, has been attributed to increased Cl- ion secretion. This increased efflux was found to be mediated by intracellular Ca^{2+} concentration and not cAMP or cGMP dependent(Canani et al., 2003). Presence of the HIV envelope protein, glycoprotein gp120, has also been shown to result in α-tubulin depolymerization and loss of *in vitro* membrane stability(Maresca et al., 2003).

When considering CFTR and CaCC, and the variety of ways in which they can be activated, it is not surprising that around 60% of patients diagnosed with HIV suffer from some form of HIV-associated diarrhea at some point during disease progression(Zingmond et al., 2003). In the past, opportunistic bacterial and/or viral infections evading destruction in the GI tract due to immune compromise could easily be attributed to acute and chronic diarrheal symptoms. Instances of opportunistic pathogenesis have decreased since the implementation of highly active antiretroviral therapy (HAART). However, several noninfectious etiologies have been identified which contribute to diarrheal symptoms. Idiopathic HIV enteropathy, autonomic neuropathy, and chronic pancreatitis are a few identified contributors to HIV-associated diarrhea. HAART-associated diarrhea has also been identified, affiliated with HIV/AIDs therapeutics such as nucleoside and non-nucleoside reverse transcriptase inhibitors, integrase inhibitors, and specifically protease inhibitors, which list diarrhea as a common side effect(MacArthur & DuPont, 2012). In vitro and human studies suggest that commonly used protease inhibitors can induce Ca^{2+} chloride channel dependent secretory diarrhea, further contributing to HIV-associated diarrhea(Rufo et al., 2004).

2.3 HIV-Associated Diarrhea Treatments and Fulyzaq®

Proper diagnosis of HIV-associated diarrhea is necessary to best prescribe effective treatment. In the case of pathogenic etiology, the specific pathogen(s) responsible should be identified and treated with appropriate antibiotics, antiparasitics, and/or antifungals. (Feasey, Healey, & Gordon, 2011). If the cause of diarrhea is non-pathogenic, such as HAART-associated diarrhea or HIV enteropathy, current treatment options are limited and only supportive in nature. Adsorbent treatments contain some form or combination of adsorbents such as attapulgite and/or bismuth subsalicylate, the active ingredients in Pepto-Bismol. Anti-motility agents are another widely used option. Drugs such as loperamide and diphenoxylate/atropine limit peristalsis of the intestine, increasing transit time allowing for increased fluid absorption. Lastly, antisecretory agents such as bismuth subsalicylate and most recently, crofelemer, have been used in alleviating HIV-associated diarrhea(MacArthur & DuPont, 2012).

Fulyzaq® is an orally dosed, enteric-coated formulation containing 125 mg of dry crofelemer API along with various excipients. Fulyzaq® is currently sold by Salix Pharmaceuticals, Inc., and was approved by the FDA in late 2012 for the symptomatic treatment of secretory diarrhea in HIV/AIDS patients taking anti-retroviral therapies, and is one of four currently approved FDA approved polymeric APIs (sevelamer, heparin, glatiramer acetate). Crofelemer acts to inhibit CFTR and CaCC channels in the GI tract, preventing excess Cl^- efflux into the luminal space. As a result, patients taking crofelemer saw a significant clinical response (17.6% taking crofelemer, 8.0% taking placebo, 1-tailed $p<0.01$). Crofelemer was shown to have very little ability to permeate the intestinal wall, and because of this its inhibition of Cl- channels is limited to the GI tract.

2.4 Introduction to Crofelemer

Crofelemer is a botanically sourced polymer refined from the stem bark latex of the *Croton lechleri* tree endogenous to South America. This red latex, commonly referred to as "Sangre de Drago" or "dragon's blood" (Figure 2) is a widely used traditional medicine for the treatment of cough and flu, diarrhea, stomach ulcers, lacerations, sores, herpes infection, and wound healing[(Ubillas et al., 1994)]. Efforts in the scientific community have been made to utilize these therapeutic properties through development of more refined versions of this latex. These fractions, most notably SP-303, were investigated for their anti-viral and anti-secretory properties through various application strategies. Eventually trademarked under the name crofelemer, SP-303 is a mixture of proanthocyanidin oligomers composed of (+)-catechin, (+)-gallocatechin, (-)-epicatechin, and (-)-epigallocatechin subunits with an average degree of polymerization of 5 to 7.5 units, but with a range from 1-28 repeating units. Among the repeating catechin and gallocatechin units are believed to be trace amounts of anthocyanidin molecules, which give crofelemer its characteristic dark red color, though these minor units have yet to be identified.

Investigations into crofelemer's anti-secretory properties determined it acts preferentially to inhibit the CFTR and CaCC chloride channels. Patch clamp and Ussing chamber studies indicate Cl- channel inhibition in a concentration dependent manner[(Fischer et al., 2004; Gabriel et al., 1999; Tradtrantip, Namkung, & Verkman, 2010)]. In one study, increasing concentrations of orally dosed, enteric-coated crofelemer resulted in decreasing amounts of intestinal fluid accumulation in 8-10 week old C57B1/6 mice when challenged with cholera toxin administration[(Gabriel et al., 1999)]. Investigations using CFTR inhibitors in combination with CaCC agonists (ATP or thapsigargin) indicate fast and almost total inhibition of CaCC Cl- ion efflux, whereas CFTR Cl- ion efflux in

the presence of the cAMP agonist forskolin only showed limited inhibition. Though washout of non-absorbable anti-secretory agents can occur in instances of diarrhea can be common, various concentrations of crofelemer were able to retain over 50% of their inhibitory effect toward CFTR challenge up to 4 hours. Co-inhibition studies with CFTR inhibitors thiazolidinone or glycine hydrazide showed non-competitive inhibition of Cl- ion efflux, suggesting different CFTR inhibition sites[(Tradtrantip et al., 2010)]. The exact mechanism of action of crofelemer for CaCC and CFTR inhibition is unknown.

Image Source: https://upload.wikimedia.org/wikipedia/commons/9/9c/Sangre_de_Grado.jpg

Figure 2: Red latex of the *Croton lechleri* tree.

2.5 Critical Quality Attributes, Mathematical Modeling, and Similarity Assessment

As a botanically sourced polymer, substantial variability in finalized crofelemer drug product can occur based on harvesting location, environmental conditions, purification and manufacturing processes. Robust, reliable analysis of crofelemer composition batch to batch is necessary to ensure its safety and efficacy before distribution and sale. In every complex biological product, certain chemical and/or physical characteristics may be more indicative of changes in safety and/or biological activity than others. These information rich features, dubbed critical quality attributes (CQAs), should be identified and monitored for comparability assessment between different lots of complex drug product. CQAs are inherent to every drug product, and proof of similarity between CQAs of innovator drugs (reference products) and potential generic forms (test products) is necessary in determining comparability as outlined by the regulatory approval processes for generic complex biological drugs which are highly dependent on manufacturing process and source of origin.

In recent years the FDA has outlined a stepwise approach toward obtaining biosimilarity or interchangeability status of a test compound. This stepwise approach focuses on acquiring a totality-of-the-evidence with which to establish proof of similarity to a reference product. This evidence starts with extensive analytical studies of both the test and reference material, in an effort to establish relevant CQAs with which to perform comparison. These CQAs are split into three tiers. The FDA recommends an equivalency test for tier 1 CQAs, which have been shown to have the most influence on clinical outcomes. An appropriate quality range should be established for CQAs which fall into tier 2 (moderate clinical impact), while graphical presentation/comparison is sufficient for tier 3 CQAs[(Chow, Song, & Bai, 2016)]. While the best statistical

methods with which to perform comparisons in each tier is still under debate, reliable and robust identification of CQAs for each biosimilarity case is an important first step in establishing regulatory approval.

By applying a machine learning approach using large amounts of physical, chemical, and biological characterization data, mathematical models that can identify information rich, product specific CQAs can be developed. Once a model has been established, it can then be applied for fast and reliable comparability assessment of generic forms against currently approved complex therapeutics, as well as batch-to-batch quality assurance. These models will assist companies developing follow-on biologics and other forms of complex pharmaceuticals to make informed decisions and identify relevant analytical assays for similarity assessment in a more cost and time efficient manner, hopefully increasing biosimilar approvals in the near future.

3. Experimental

3.1 Materials

Fulyzaq® tablets (Silax Pharmaceuticals, Lot #s 3118488, 3117608, and 3128292) were acquired from local pharmacies (Sigler Pharmacy, WE Pharma). Deuterium oxide (D_2O) was purchased from EMD Millipore Corporation (Billerica, MA, USA). Double distilled water (ddH_2O) was used for buffer preparations, while ultrapure water was used for preparation of crofelemer samples for use in all bioassays. Amicon® Ultra-15 3 kDa and 10 kDa MWCO centrifuge filters were purchased from Merck Millipore Ltd. (Tullagreen, Carrigtwohill Co. Cork, Ireland). Wilmad 500 MHz thin wall NMR tubes were purchased from Milmad LabGlass (Vineland, NJ, USA). T84 cells (passage 55) were purchased from the American Tissue Culture Collection (ATCC, Manassas, VA, USA). DMEM:F12 media + L-Glutamine and 2.438 g/L sodium bicarbonate was purchased from Life Technologies (Grand Island, NY, USA). Fetal bovine serum (FBS) was purchased from Atlanta Biologicals (Atlanta, GA, USA). A 0.25% Trypsin, 2.21 mM EDTA solution was purchased from Mediatech, Inc. (Manassas, VA, USA). N-(Ethoxycarbonylmethyl)-6-Methoxyquinolinium Bromide (MQAE) was purchased from Biotium, Inc. (Hayward, CA, USA). Forskolin and Ionomycin were purchased fro LC Laboratories (Woburn, MA, USA). Quercetin was obtained from Sigma Aldrich (St. Louis, MO, USA). Ethanol, 190 Proof, was purchased from Decon Laboratories, Inc. (King of Prussia, PA, USA). Buffer salts used in chloride channel assays were obtained from Fisher Scientific (Fair Lawn, NJ, USA). Costar 3603, Black, clear bottom tissue culture treated 96 well plates and 75 cm^2 vented tissue culture flasks were purchased from Corning, Inc. (Corning, NY, USA).

3.2 Methods

3.2.1 Fulyzaq® API Extraction

The enteric coating of Fulyzaq® tablets (consisting of ethylacrylate and methylacrylate copolymer dispersion, talc, triethyl citrate, and a white dispersion composed of xanthan gum, titanium dioxide, propyl paraben, and methyl paraben) was carefully removed using a clean razorblade. The packed pill containing a mixture of 125 mg of crofelemer dispersed in insoluble excipients (microcrystalline cellulose, croscarmellose sodium, colloidal silicon dioxide, and magnesium stearate) was gently crushed into a powder. Crofelemer and excipients were then dissolved directly into 5 mL/pill of ultrapure H_2O (or D_2O for NMR samples) and vortexed to yield a 25 mg/ml solution of crofelemer. The dissolved drug and excipient suspension was centrifuged at 3,700 xg for 1 hour, and the supernatant was collected. Unfractionated samples were aliquoted and either tested immediately, frozen (-80ºC), or incubated at controlled temperatures for forced degradation studies.

3.2.2 Crofelemer Fractionalization and Forced Degradation of Samples

Crofelemer was fractionated using 3-kDa and 10-kDa molecular weight cut-off (MWCO) centrifuge filters. A 10 mL solution (25 mg/ml) of unfractionated crofelemer was added to the top of the respective centrifugal filters and centrifuged at 4,000 xg for 30 minutes on an accuSpinTM 3R swing bucket centrifuge (Fisher Scientific, Fair Lawn, NJ). Concentrate was diluted with ddH_2O (or D_2O for NMR samples) back to 10 ml and centrifuged under the same conditions a second time. Concentrate was again diluted to 10 ml. Aliquots of concentrate, deemed “Top” and filtrate, deemed “Bottom” were then prepared alongside unfractionated samples. NMR samples (unfractionated and Top fractions) were stored at 25 mg/ml at their

respective temperatures (25ºC and 40ºC) in a controlled environment until time-points were reached, at which point spectra were either collected immediately or samples were frozen until readings could be taken. Top and unfractionated crofelemer samples for biological testing were first diluted to 0.5 to 0.4 mg/ml before preparing aliquots. Time zero samples were frozen immediately (-80ºC) while degradation samples were stored at their respective temperatures (25ºC and 40ºC) alongside NMR samples. Bioassays of degraded samples were tested as time-points were reached, or samples were frozen until assays could be performed. Table 1 summarizes the tested sample temperatures and time points.

Table 1: Forced degradation sample temperatures and time-points tested.

	Unfractionated, 10 kDa Top, and 3 kDa Top Samples				
		25ºC		40ºC	
	Time Zero	7 day	30 day	7 day	30 day
T84 Assay					
^{1}H NMR and Quantitative ^{13}C NMR		NT*		NT	

* NT: not tested

3.2.3 ^{1}H and Quantitative ^{13}C NMR of Forced Degradation Samples

^{1}H NMR spectra of (+)-catechin, epigallocatechin gallate, and crofelemer samples were obtained using an Avance 400 MHz NMR (Bruker, MA) spectrometer. A total of 128 scans were collected per ^{1}H NMR sample. Quantitative ^{13}C NMR spectra of crofelemer samples were

collected using an Avance AVIII 500 MHz NMR spectrometer (Bruker, MA) equipped with a dual carbon/proton (CPDUL) cryoprobe, using a zgig pulse program, 3200 scans, with a 25 second interscan delay. All samples were dissolved in D_2O. One-month incubated samples (25°C and 40°C) showed visual evidence of precipitation and were centrifuged for 15 min at 14000 x g in a Sorval Legend Micro 17 Centrifuge (Thermo Scientific, US) to exclude particulates before spectra were recorded. Spectra were manually phase corrected and appropriately baseline corrected using MestRe Nova 9.0 (Mestrelab Research, S. L.) before data analysis. Previously reported ^{13}C NMR shift values for crofelemer are shown in Figure 3[(Ubillas et al., 1994)].

The internal/terminal unit ratio (IU / TU) of each sample was calculated through integration of the C-4 δ 36.35 and δ 38.24 ppm signals of internal units and the δ 28.67 signal of its terminal unit counterpart. The ratio of 2,3-trans and 2,3-cis species within samples was determined through integration and comparison of the C-2 δ 82.9 ppm signal characteristic of the catechin and gallocatechin (2,3-trans) moieties, and the C-2 δ 76.6 ppm signal characteristic of the epicatechin and epigallocatechin (2,3-cis) moieties. The procyanidin (PC) and prodelphinidin (PD) composition of crofelemer could be estimated due to slight variations in signal contributions to the δ 146.2 ppm and δ 131.4, 133.9 ppm signals attributed to the B ring of the repeating units. Both catechin and gallocatechin units have two carbons which contribute to the δ 146.2 signal seen in the ^{13}C-NMR spectra, however catechin units only possess one carbon which contributes signal at around δ 133.9 ppm, while gallocatechin units have both a carbon that contributes to the δ 133.9 signal as well as a carbon which has a δ 131.4 ppm shift. We utilized this difference in signal contribution, along with the ratio of ~146 and ~131-133 signal ranges to determine the different contributions of both PC and PD moieties within the total

crofelemer sample. When applied to the normalized function for PC and PD contributions, we could calculate the percent composition of PC and PD within a sample:

$$Signal_{146ppm} = 2PC + 2PD = 1\ (normalized)$$

$$PD = 0.5 - PC$$

$$Signal_{132ppm} = PC + 2PD = AUC\ relative\ to\ Signal\ at\ 146ppm$$

$$\frac{Signal_{132ppm}}{Signal_{146ppm}} = \frac{PC + 2(0.5 - PC)}{2PC + 2(0.5 - PC)} = \frac{AUC\ relative\ to\ Signal\ at\ 146ppm}{1\ (normalized)}$$

$$\mathrm{PC} = 1 - AUC\ relative\ to\ Signal\ at\ 146ppm$$

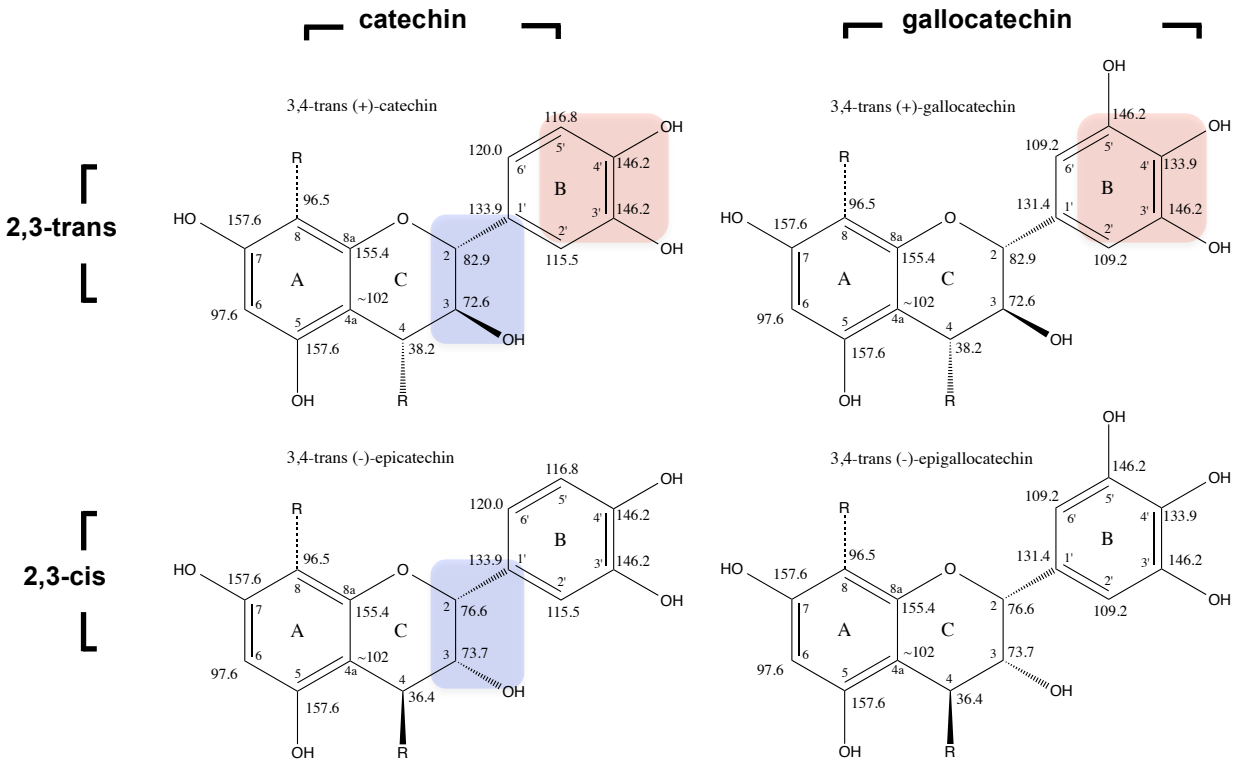

Figure 3: ^{13}C NMR shift values for the repeating units of crofelemer[(Ubillas et al., 1994)]. Changes in C2 and C3 signals indicating trans and cis forms are highlighted in blue. Varying contributions to the δ 133.9 ppm signal from catechin and gallocatechin moieties are highlighted in red.

3.2.4 T84 Chloride Channel Inhibition Assay

T84 chloride channel inhibition assays were performed using a method adapted from West and Molloy [(West & Molloy, 1996)]. T84 cells were maintained using 1:1 DMEM/F12 culture media with L-Glutamine and 2.438 g/L sodium bicarbonate supplemented with 5% (v/v) FBS in a controlled 5% CO_2 atmosphere at 37ºC. Cells were initially plated onto T-75 tissue culture flasks and passaged at least twice before use in fluorescence assays. Cells were seeded onto 96 well plates at a density of $2x10^4$ cells/well, and culture media was changed every two days until all wells reached confluence. A 10-mM solution of the Cl^- quenched fluorescent probe MQAE dissolved in 100 µL culture media was administered to each cell monolayer for 10 hours prior to sample testing.

After MQAE incubation, culture media was removed and replaced with a Cl^- containing buffer solution (buffer 1) (65mM NaCl, 1.2mM K_2HPO_4, 0.3 mM KH_2PO_4, 0.5 mM $CaSO_4$, 0.5 mM $MgSO_4$, 5mM HEPES, 5mM Dextrose, pH 7.4). Monolayers were washed twice for 10 minutes with 150 µL/well fresh buffer 1 on a ZD-9556-A Orbital Shaker (Madell Technology Corp, CA) at 65 rpm to establish intracellular/extracellular equilibrium Cl^- concentration. Monolayers were then exposed to freshly prepared solutions of either 100 µM quercetin in buffer 1 (positive control), 0.1 mg/ml crofelemer in buffer 1, or buffer 1 alone (negative control) for 5 minutes. After 5 minutes, buffer 1 solutions were removed and replaced with 0.1 mg/ml crofelemer samples, alone and in the presence of either 10µM forskolin or 10µM ionomycin to challenge crofelemer's ability to inhibit Cl^- efflux. Crofelemer samples, with or without forskolin or ionomycin, were dissolved in Cl^- free buffer (buffer 2) (65mM $NaNO_3$, 1.2mM K_2HPO_4, 0.3 mM KH_2PO_4, 0.5 mM $CaSO_4$, 0.5 mM $MgSO_4$, 5mM HEPES, 5mM Dextrose, pH 7.4), along with respective positive and negative controls. Quercetin, forskolin and ionomycin were

insufficiently soluble in buffer solutions alone and were presolubilized in 26 µl of 95% ethanol. Fluorescence measurements were taken immediately in 25-second intervals for 25 min, λ_{ex} = 360 nm λ_{em} = 460 nm. Figure 4 summarizes the steps involved in the microplate assay. Changes in fluorescence were determined by subtracting the time-zero relative fluorescence units (RFU) from subsequent measurements (Ft-F0), and curves were normalized between quercetin and blank controls for sample comparison. Samples were tested on three separate 96 well plates, eight wells per sample group per plate, for a total of 24 wells per sample group. All assays were carried out at room temperature (22ºC).

Forskolin and ionomycin were first tested on T84 monolayers to ensure their ability to initiate Cl^- channel efflux of their respective ion channels, CFTR and CaCC. The concentration of crofelemer tested was based on previous patch clamp and Ussing chamber studies involving Cl^- measurement[(Gabriel et al., 1999; Tradtrantip et al., 2010)]. Concentrations of forskolin and ionomycin were based on those used previously for assessing Cl- ion efflux in T84 monolayers[(Gabriel et al., 1999; West & Molloy, 1996)].

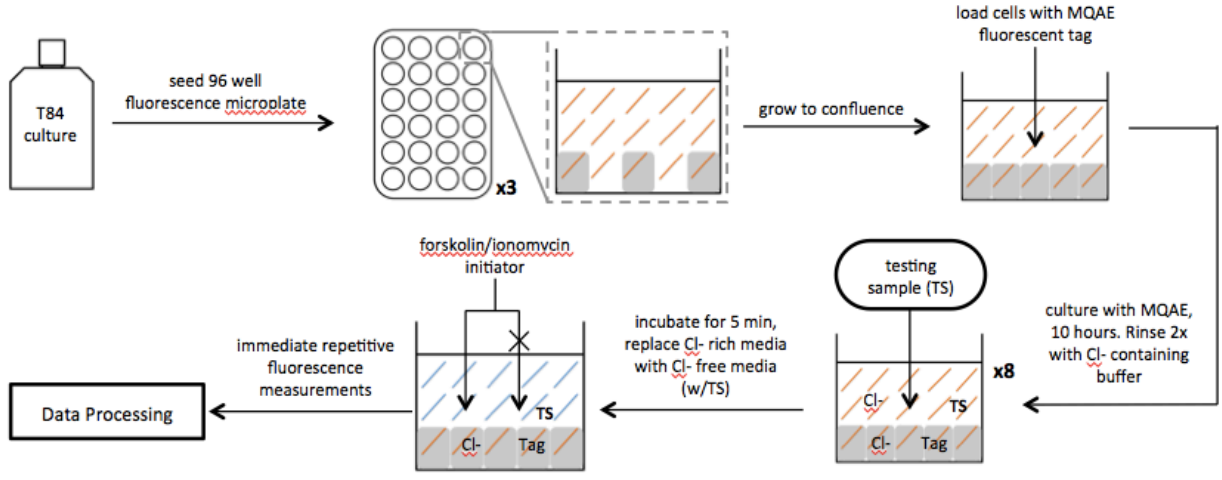

Figure 4: Workflow diagram outlining T84 chloride channel assay.

3.2.5 Initial Lot Variability Investigation

Since crofelemer is not a synthetically manufactured compound but rather a harvested ethnobotanical drug, there is inherent variation between lots of released drug product. Triplicate ^{1}H NMR and qCNMR spectra were collected as reported earlier for three different lots; Lot 1 (3118488), Lot 2 (3117608), and Lot 3 (3125951), to first confirm differences in observable characteristics. The ^{1}H NMR of mixture samples were collected using an Avance AVIII 500 MHz NMR spectrometer (Bruker, MA) equipped with a dual carbon/proton (CPDUL) cryoprobe, 16 scans.

3.2.6 Mixture Studies

Once batch-to-batch variability was confirmed, unfractionated samples of individual lots were then mixed together to form six artificial lots whose compositions are listed in Table 2. By mixing these lots in various ways, artificial lots with subtle variations were produced with which to test and further refine the mathematical model and CQA selection process.

Table 2: Compositions of mixtures produced from the three different crofelemer lots. Values represent % compositions of each mix.

Sample	Mix 1	Mix 2	Mix 3	Mix 4	Mix 5	Mix 6
Lot 1	10	10	33.3	-	-	-
Lot 2	90	-	33.3	50	10	90
Lot 3	-	90	33.3	50	90	10

4. Results

4.1 NMR Characterization

4.1.1 Initial NMR Studies

Initially, ^{1}H NMR were collected for two compounds representative of crofelemer's monomeric units, (+)-catechin (Figure 5) and epigallocatechin gallate (Figure 6). The (+)-catechin sample possesses two sets of doublets (δ 2.514, 2.534 ppm and δ 2.555, 2.574 ppm) for the C4-β proton and two sets of doublets (δ 2.848, 2.861 ppm and δ 2.888, 2.902 ppm) for the C4-α proton. A sextet (δ 4.198, 4.211, 4.217, 4.230, 4.236, 4.250 ppm) is observed for the proton located on C3. Signal from the C2 proton was obfuscated by the H_2O impurity of the solvent. The A8 and A6 protons both displayed doublets (δ 6.017, 6.023 ppm and δ 6.100, 6.105 ppm respectively). The B2', B5', and B6' proton shifts fell on the range of δ 6.851 to 6.949 ppm.

The epigallocatechin gallate sample possesses two sets of doublets (δ 2.863, 2.868 ppm and δ 2.907, 2.913 ppm) for the C4-α proton and two sets of doublets (δ 2.969, 2.980 ppm and δ 3.012, 3.024 ppm) for the C4-β proton. A singlet is present at δ 5.013 ppm. What appears to be a quintet (δ 5.528, 5.532, 5.537, 5.542, 5.547 ppm) can most likely be attributed to the C3 proton. Signal contributions from the A6 and A8 protons can be seen from δ 6.094 to 6.127 ppm. A strong singlet is present at δ 6.547 due to contributions of the B2' and B6' protons. Another strong singlet can also be seen at δ 6.956 ppm from the 2" and 6" proton signals. The shift values correspond well with previously published shift values of (+)-catechin and epigallocatechin gallate in d_6-acetone[(Davis, Cai, Davies, & Lewis, 1996)].

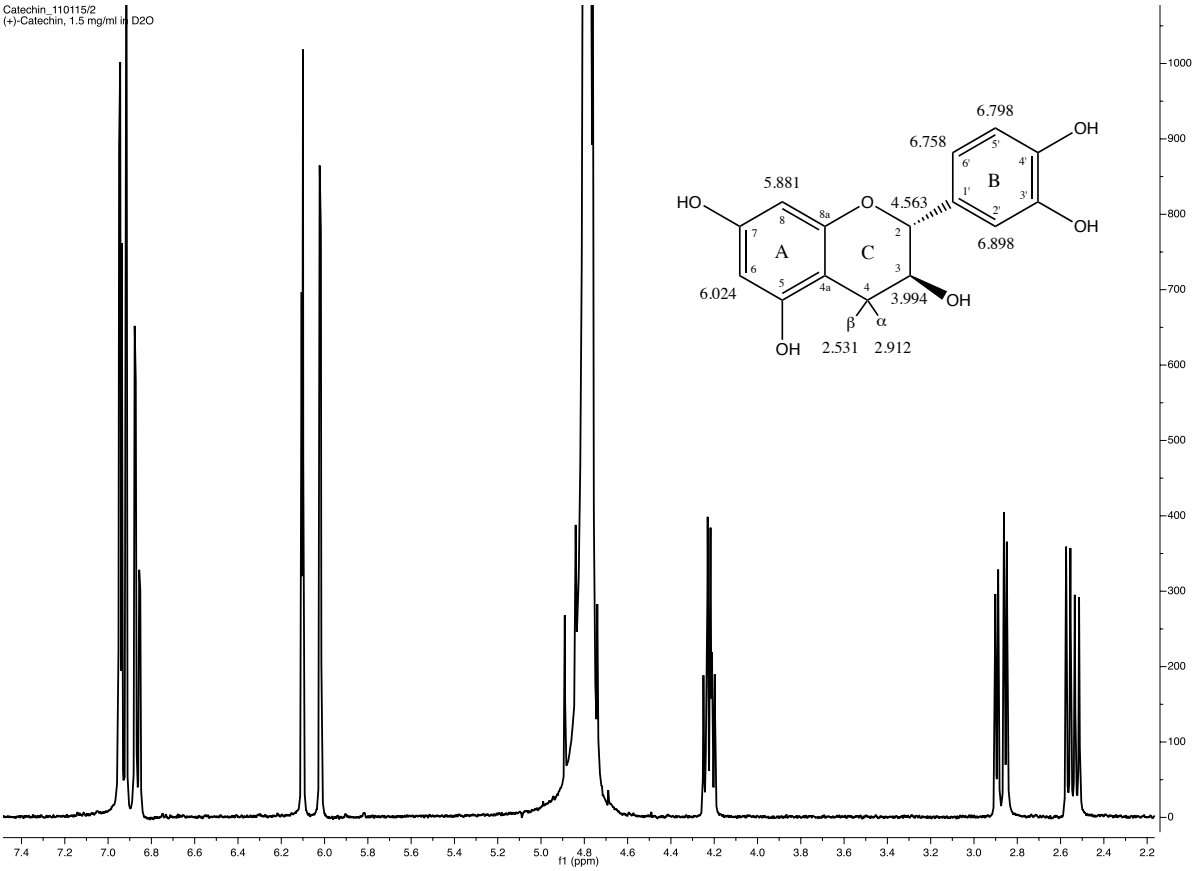

Figure 5: ^{1}H NMR spectrum of (+)-catechin in D_2O. Shift values correlate well with those published previously for (+)-catechin in d_6-acetone, shown with corresponding structure[(Davis et al., 1996)].

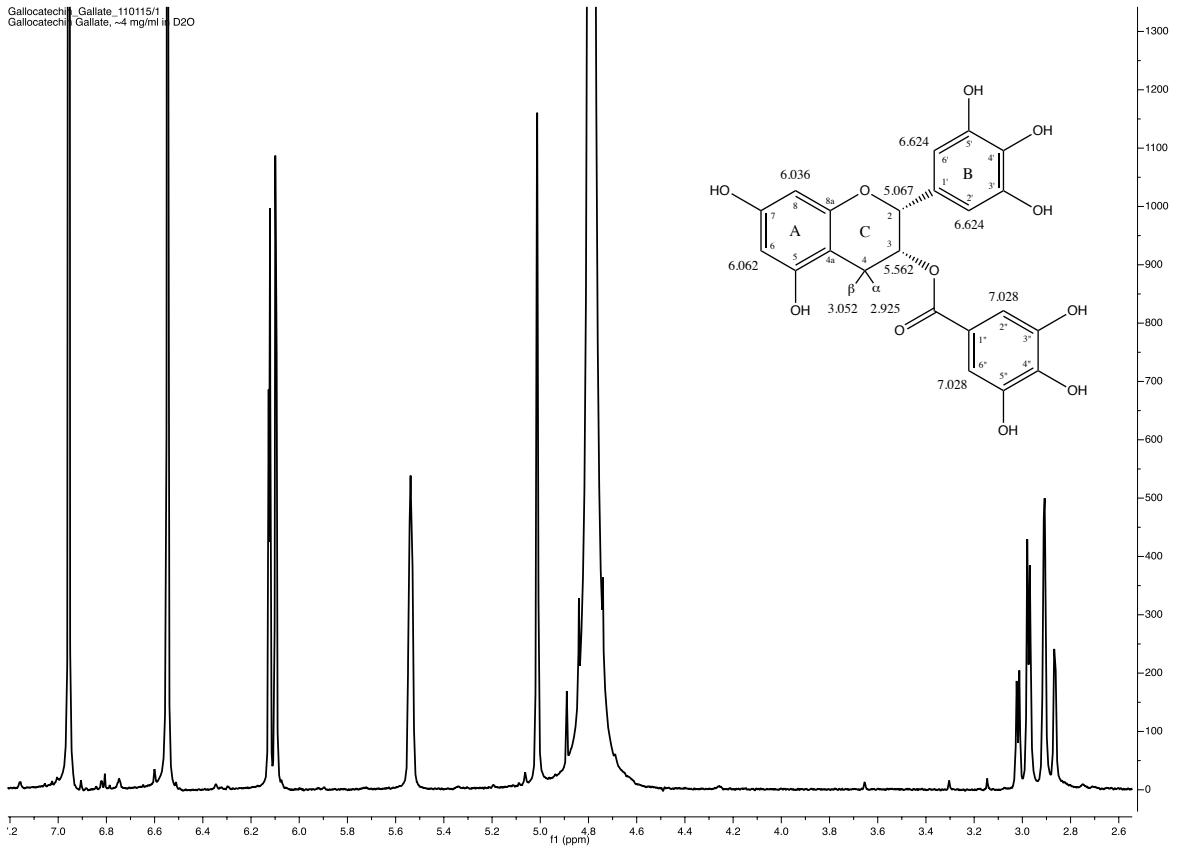

Figure 6: ^{1}H NMR spectrum of epigallocatechin gallate in D_2O. Shift values correlate well with those published previously for epigallocatechin gallate in d_6-acetone, shown with corresponding structure[(Davis et al., 1996)].

4.1.2 ^{1}H and Quantitative ^{13}C NMR of Forced Degradation Samples

The NMR spectra of crofelemer is not publically available, however there are published peak assignments for the precursor to crofelemer, SP-303. Ubillas et. al. reported broad peaks from δ 2.2-3.0, 3.2-5.4, and 5.5-7.3 ppm in their 1H NMR spectra of SP-303. ^{13}C NMR of SP-303 also contained broad peaks at δ 28.7, 36.4, 38.2, 66.7, 72.6, 73.7, 76.6, 78.8, 82.9, 96.5, 97.6, 107.4, 109.2, 115.5, 116.8, 120.0, 121.1, 131.4, 133.9, 146.2, 155.4, and 157.6. Proton NMR spectra for the first available lot of crofelemer (Lot 3118488) show broad peaks in the ranges of δ 2.0-3.1, 3.1-5.5, and 5.5-7.3 ppm. Quantitative ^{13}C spectra for crofelemer possess broad peaks at δ 28.67, 36.35, 38.24, 66.69, 72.43, 73.83, 76.57, 78.79, 82.90, 96.44, 97.91, 107.59, 109.13, 155.53, 116.44, 117.19, 120.22, 121.20, 121.96, 131.18, 131.64, 132.55, 133.92, 144.45, 146.25, 155.32, and 157.55 ppm.

^{1}H NMR spectra for day 0 unfractionated, 10 kDa top, and 3 kDa top samples (Lot CF3117608) showed no change in peak positions (Figure 7). Sharp peaks (δ 3.5 to 3.8 ppm) present in the 10 kDa and 3 kDa MWCO filtered samples are characteristic of cellulose that contaminated the sample during centrifugal filtration. The day 30 unfractionated samples incubated at 25°C and 40°C displayed a broadening of any distinguishable characteristics present in the peaks of day 0 samples, with a significant decrease in overall signal intensity in the 40°C samples (Figure 8).

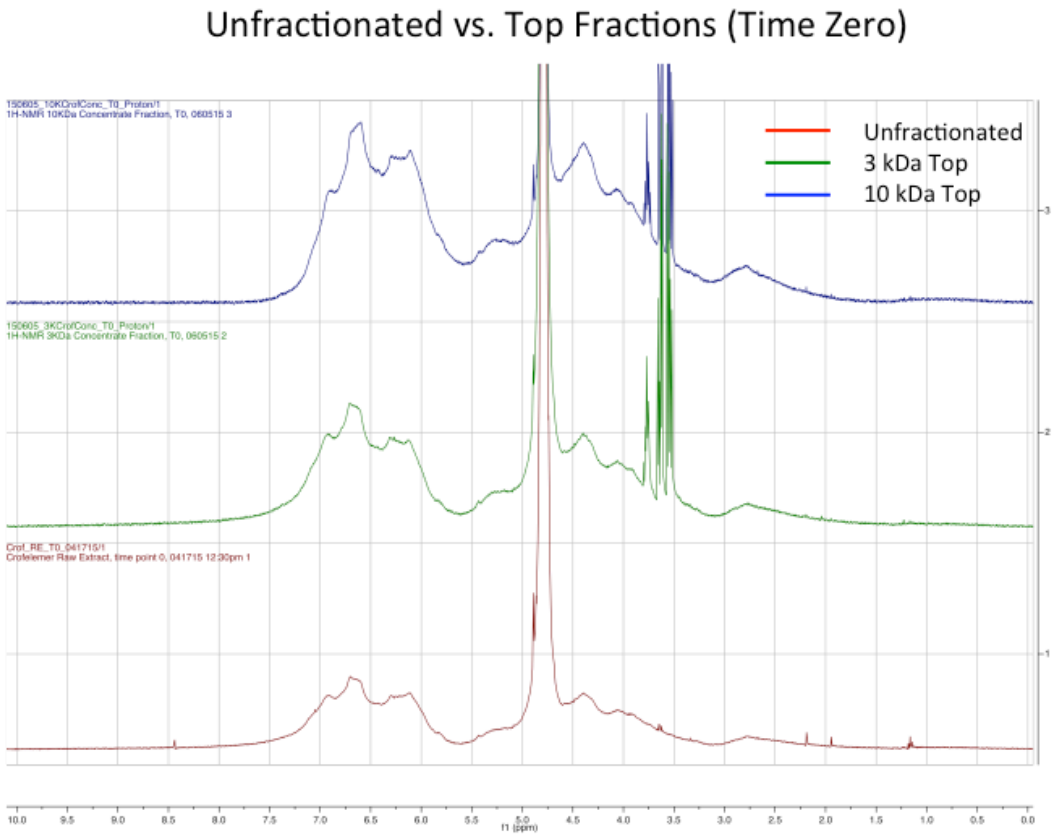

Figure 7: 1H-NMR Comparison of unfractionated, 10 kDa top, and 3 kDa top crofelemer samples. No substantial differences were observed across the unfractionated and top fraction crofelemer samples. The presence of sharp peaks (δ 3.5 to 3.8 ppm) in the 10 kDa top and 3 kDa top fractions are characteristic of cellulose contamination from the centrifugal filters[(Isogai, 1997)].

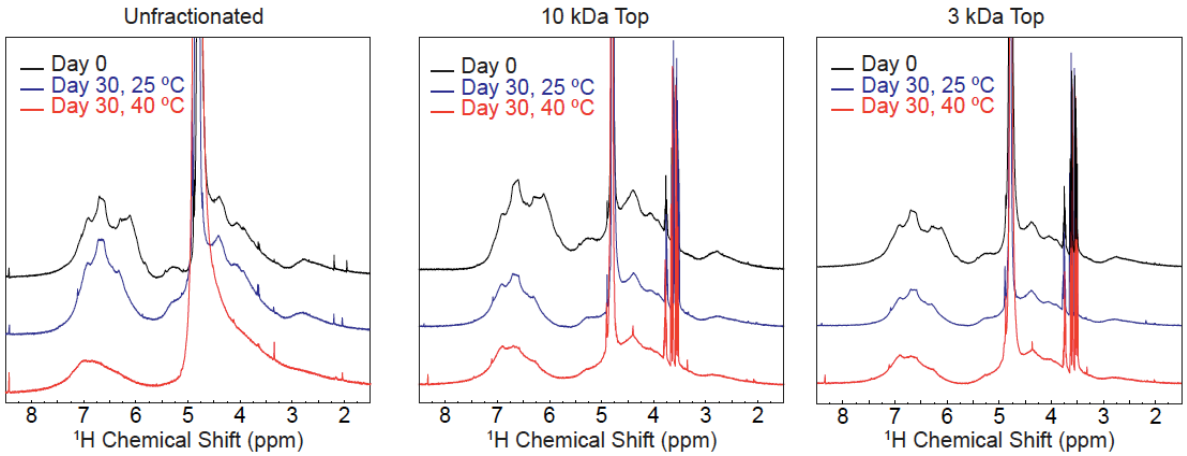

Figure 8: ^{1}H-NMR comparison of day 0 and 25°C, 40°C day 30 crofelemer samples. Smoothing of characteristic features and decrease in signal magnitude occurred during the 30 day degradation period.

For qCNMR analysis of the crofelemer samples, the overall positioning of peaks in the ^{13}C-NMR did not change throughout sample degradation. However, changes in peak intensities, as well as broadening of peaks resulted in detectable changes in peak integration and ratio determinations, which are indicative of chemical changes occurring within the sample entirety over time (Figure 9).

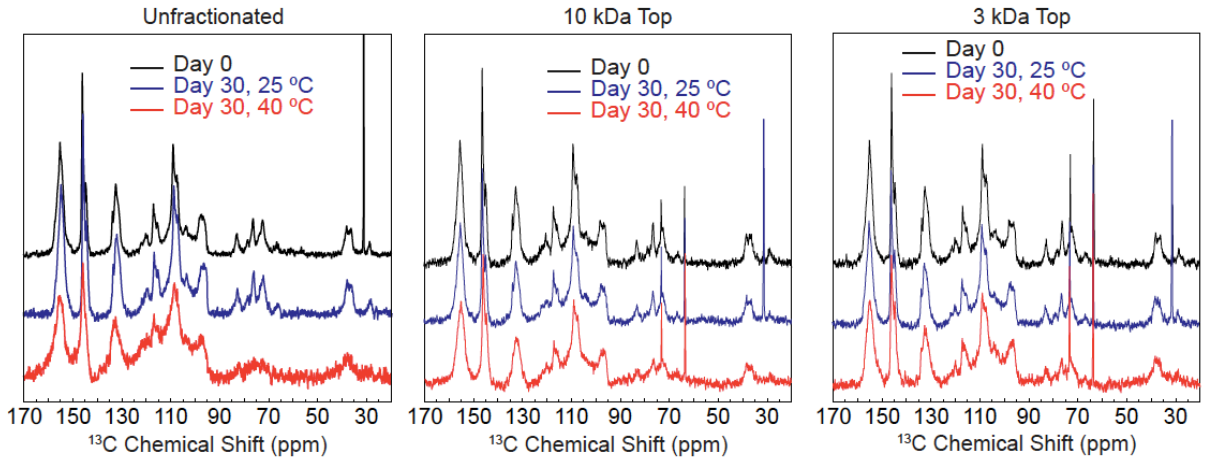

Figure 9: Quantitative ^{13}C-NMR comparison of day 0 and 25°C, 40°C day 30 crofelemer samples. Precipitation of sample over the 30 day period contributed to signal loss in the 40°C samples, making some sample IU/TU ratios unreliable. Residual acetone from the NMR tube was present in the unfractionated day 0 sample, as well as the 10 kDa top and 3 kDa top day 30 25°C degree samples. The signal contribution of the δ 31.2 ppm contaminant peak has been excluded in analysis of proximal peaks.

Peaks of interest for determining IU/TU, Trans/Cis, and PC% and PD% were integrated and respective values for each sample can be found in **Table 3**.

Table 3: Differences in IU/TU, Trans/Cis, and PC/PD Ratios for Crofelemer Samples as Determined by qCNMR.

Sample	Trans/Cis	PC%	PD%	IU/TU
Unfractionated, T0	0.69	31.16	68.84	6.76
Unfractionated, 30 Day 25℃	0.82	34.51	65.49	4.93
Unfractionated, 30 Day 40℃	IS*	50.54	49.46	IS*
10kDa Top, T0	0.72	33.52	66.48	4.27
10kDa Top, 30 Day 25℃	0.72	24.88	75.12	4.87
10kDa Top, 30 Day 40℃	0.64	72.58	27.42	4.53
3kDa Top, T0	0.58	23.60	76.40	3.79
3kDa Top, 30 Day 25℃	0.73	47.33	52.67	3.61
3kDa Top, 30 Day 40℃	0.77	43.02	56.98	4.27

* IS: insufficient signal

Day 0 unfractionated crofelemer had an IU/TU ratio of 6.76, resulting in an estimated number average molecular weight of 2,328 g/mol. An unexpected decrease in molecular weight was seen in the top fractions of both 10 kDa and 3 kDa MWCO centrifuge filters used, with estimated average molecular weights of 1,581 g/mol and 1,437 g/mol, respectively. A decrease in the IU/TU ratio was observed in the unfractionated sample after 30 days of incubation at 25°C relative to its corresponding day 0 counterpart due to an increase in terminal unit signal relative to total signal spectra, suggesting formation of terminal units through degradation of higher molecular weight species. Accurate integration of the δ 36.4, 38.2 ppm and 28.7 ppm peaks in the 30 day, 40°C unfractionated crofelemer sample was not possible, most likely due to sample loss by precipitation and more extensive physical and/or chemical degradations. Both 3 kDa and 10 kDa top fractions showed slight increases in the IU/TU ratio for their 40°C, 30 day counterparts when compared to time zero values.

The trans/cis ratio increased from time zero values in the unfractionated and 3 kDa top fraction samples when compared to 30 day time points. These samples show a slight increase in the epicatechin and epigallocatechin population, reflected by a relative increase in the δ 76.6 ppm signal when normalized to total signal of the spectrum. However 10 kDa top fractions showed very little change in trans/cis ratio, with relatively consistent signal contributions from both δ 76.6 and 82.9 ppm.

The PC and PD percentages showed consistent trends across all three samples. Increases in PC% can be seen in unfractionated, 3 kDa and 10 kDa top fractions due to slight increases in δ 146.2 ppm relative signal contribution along with decreased contributions from the δ 131-133 ppm range. Excluding the 30 day 10 kDa top 25°C sample, every 30 day sample showed decreased relative signal from δ 131.4 and 133.9 ppm peaks, indicative of loss of the B-5' hydroxyl of gallocatechin repeating units.

4.2 T84 Chloride Channel Inhibition Assay

Forskolin and ionomycin, at concentrations of 10 μM in buffer 2, were sufficient to induce marked efflux of Cl- ion from T84 monolayers when compared to buffer 2 alone (Figure 10). Forskolin produced a more rapid net efflux with a faster initial rate when compared to ionomycin and blank control. Surprisingly, ionomycin showed a slower initial rate of efflux when compared to blank control, however after 9.5 minutes fluorescence values exceeded those of the buffer alone, and continued to increase for the remainder of the experiment.

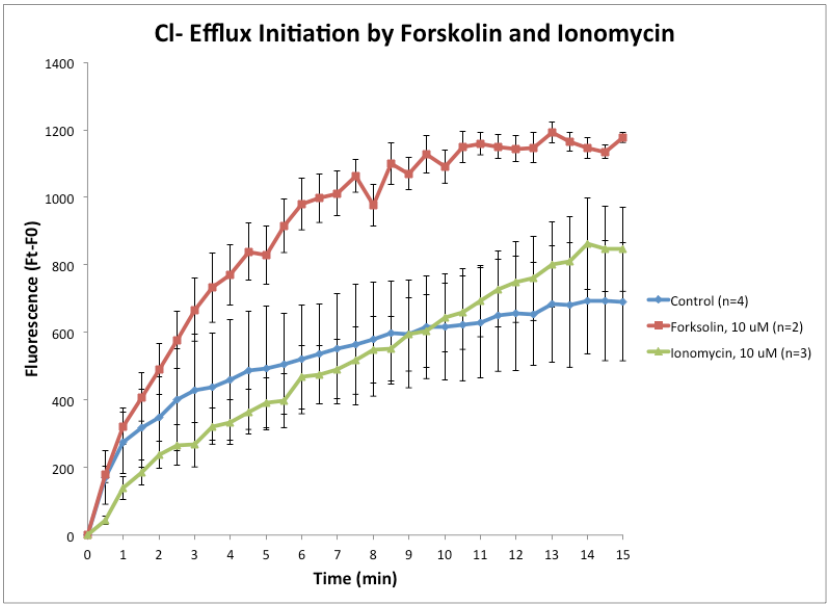

Figure 10: Initiation of Cl^- ion efflux by 10 µM forskolin and ionomycin compared to buffer absent of any Cl^- channel agonists.

All samples of crofelemer tested were able to inhibit Cl^- ion efflux from T84 cells, regardless of fractionalization, time, and temperature. Though there was visual evidence of variability between crofelemer time zero samples and their 7 and 30 day degraded forms, Cl^- efflux levels persisted below passive Cl^- efflux in every case. Fluorescence values for crofelemer samples when challenged by either ionomycin or forskolin also remained below blank control in all cases. Challenge with forskolin showed visibly higher Cl^- efflux compared to crofelemer challenged by ionomycin and crofelemer alone, showing similar behavior to initial tests with initiators alone. Overall chloride efflux behavior when cells were stimulated with ionomycin varied across samples; however, fluorescent values remained at or slightly above Ft-F0 values for crofelemer alone. Fluorescence values for crofelemer were consistently above values seen for quercetin after 25 minutes, indicating that saturation of Cl^- channels did not occur (Figure 11, Figure 12, Figure 13).

Fractionalization of crofelemer using 10 kDa and 3 kDa MWCO centrifuge filters had no noticeable effect on crofelemer's ability to inhibit Cl^- ion efflux, alone or when challenged with forskolin or ionomycin (Figure 14).

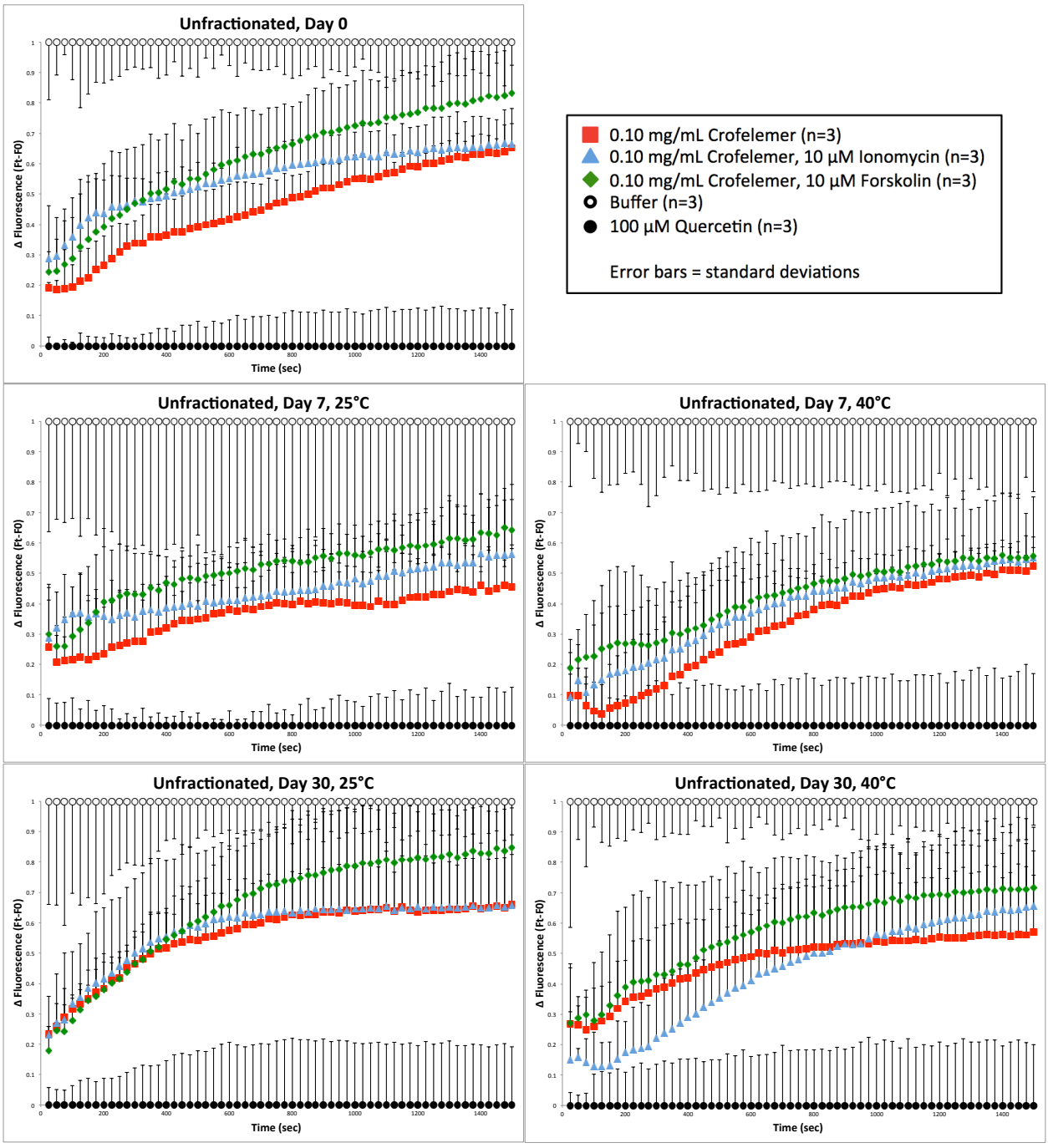

Figure 11: Total chloride ion efflux from monolayers in the presence of unfractionated crofelemer samples.

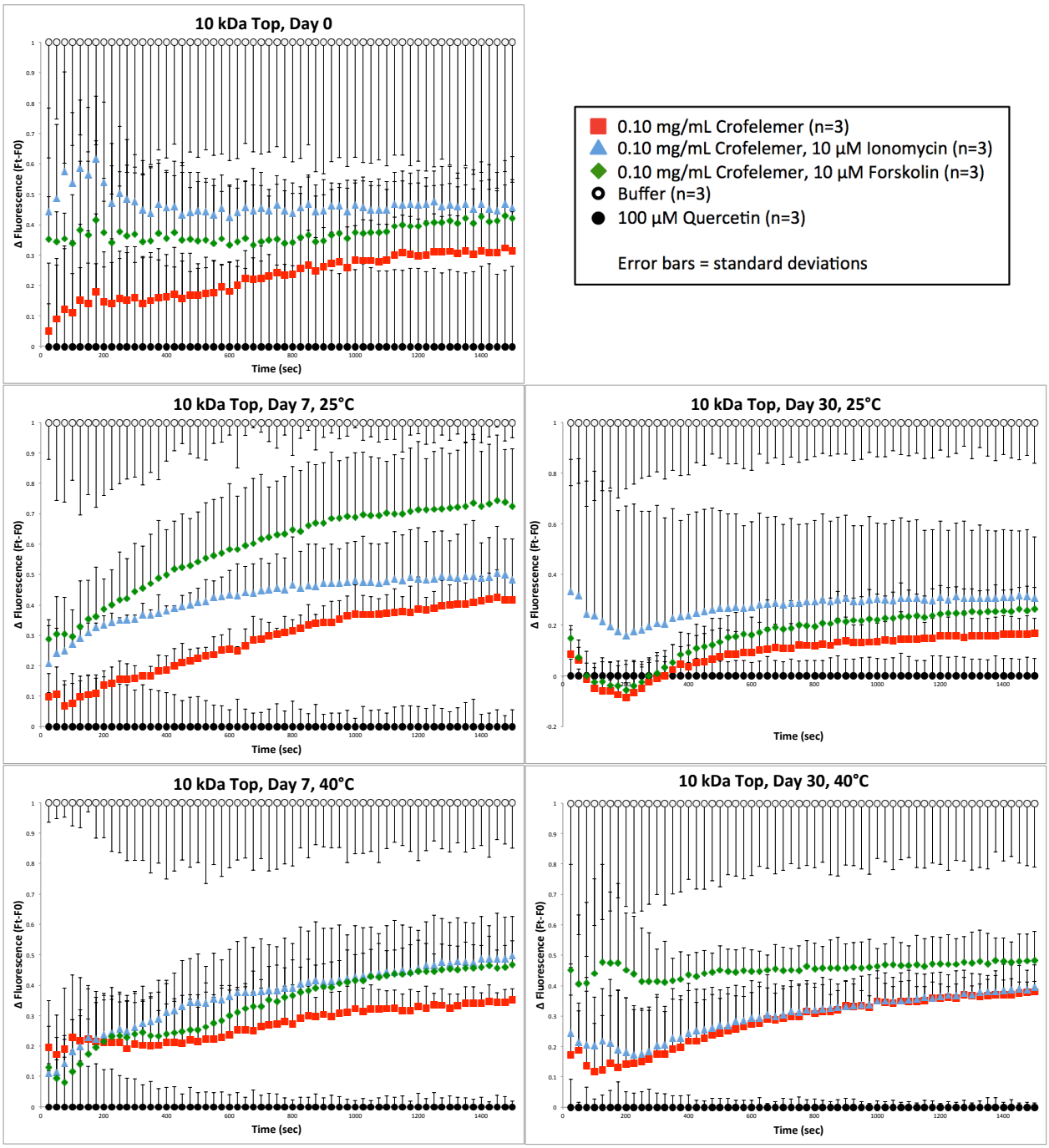

Figure 12: Total chloride ion efflux from monolayers in the presence of 10-kDa Top crofelemer samples.

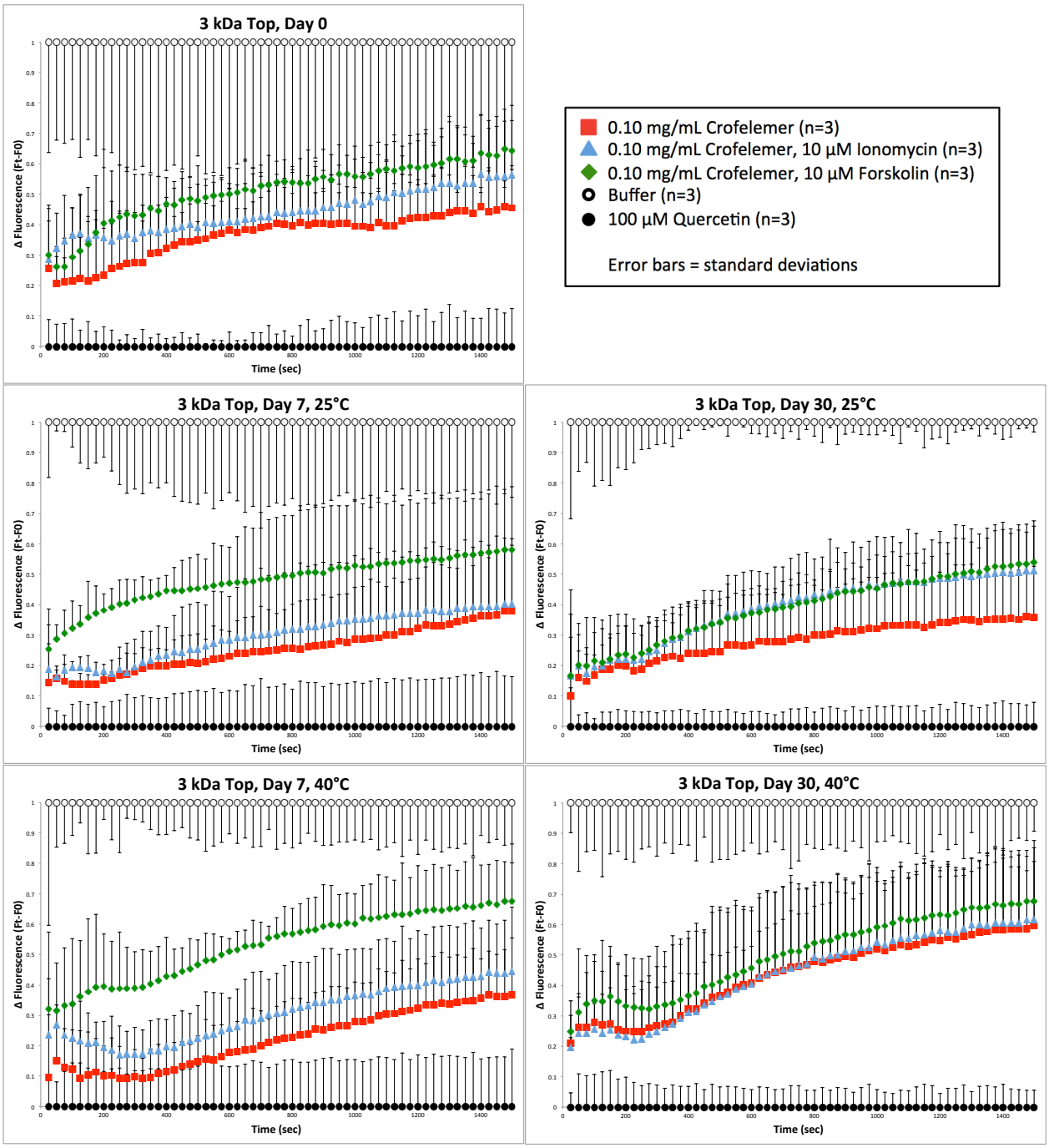

Figure 13: Total chloride ion efflux from monolayers in the presence of 3-kDa Top crofelemer samples.

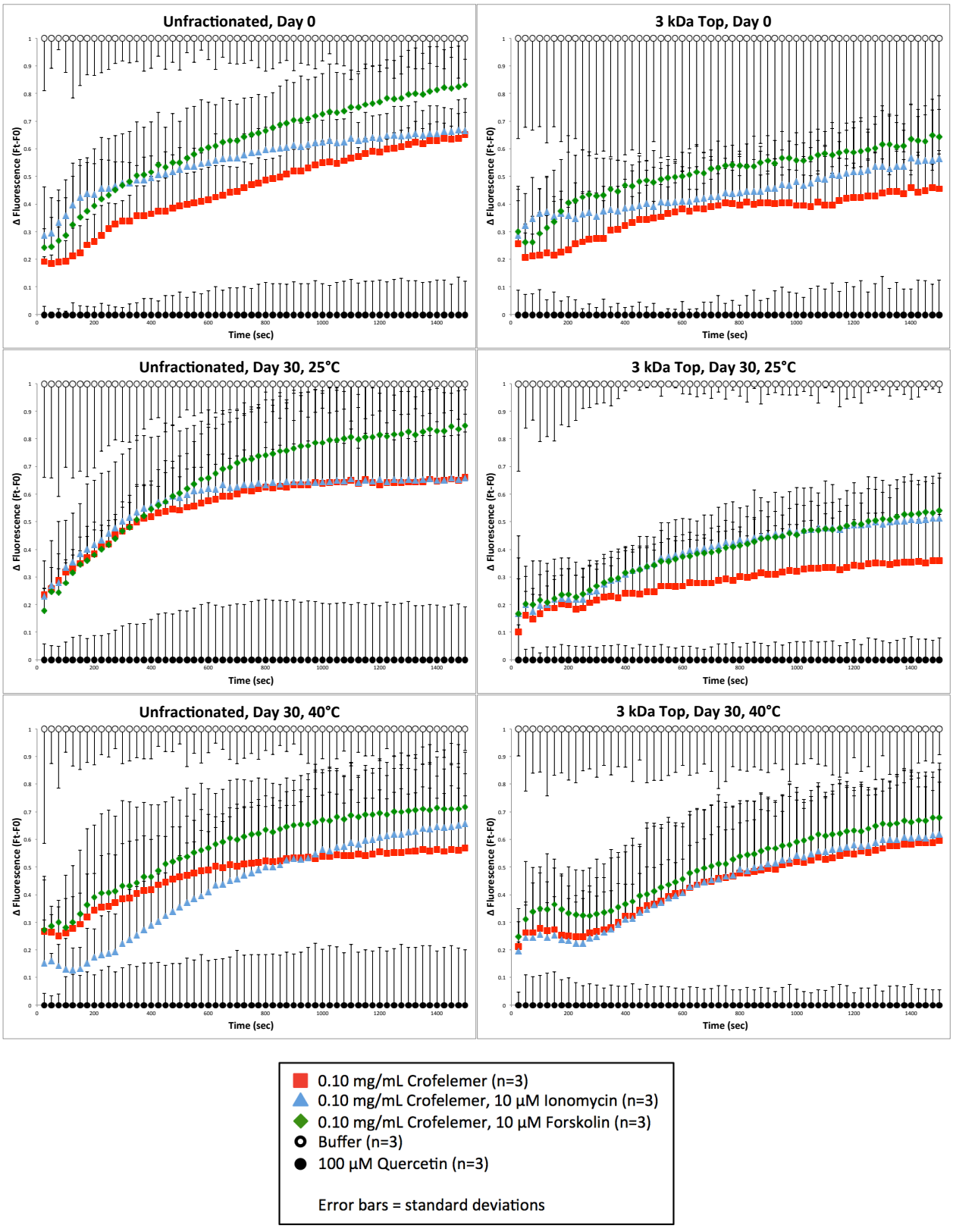

Figure 14: Comparison of unfractionated crofelemer samples to corresponding 3-kDa Top fraction samples.

4.3 Initial Lot Variability Investigation

Three separate batches of unfractionated crofelemer were acquired and analyzed in an effort to distinguish variability between different lots. Initial qCNMR studies confirmed variation in IU/TU ratios, trans/cis ratios, and PC and PD composition across the three lots tested; Lot #311848 labeled "Lot 1" (Figure 15, Table 4), Lot #3117608 labeled "Lot 2" (Figure 16, Table 5), and Lot # 3125951 labeled "Lot 3" (Figure 17, Table 6). Lot 1 possessed the highest trans/cis ratio (1.209) amongst the three lots tested, with a comparable IU/TU (3.88) to that of Lot 2. Lot 3 showed the highest IU/TU ratio (5.45) of the lots, with a comparable trans/cis ratio (0.672) to that of Lot 2. The PC and PD compositions across the three lots were similar, with a majority of prodelphinidin moieties. Differences in PC and PD compositions, IU/TU, and trans/cis ratios between the three lots are summarized in Table 7.

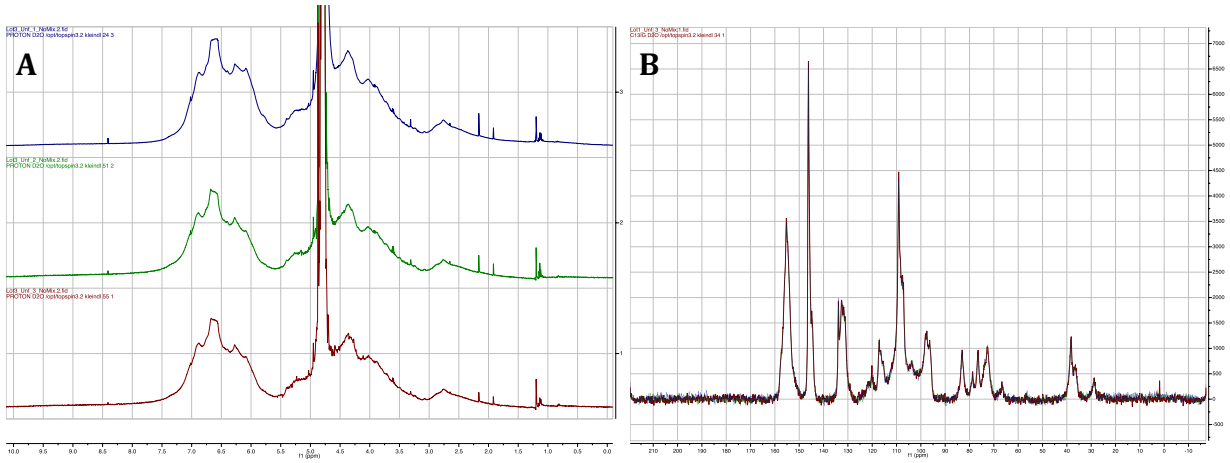

Figure 15: Triplicate spectra of Lot 1 (3118488). A) 1H NMR spectra. B) Overlaid qCNMR spectra.

Table 4: Calculated values of interest for Lot 1 (3118488) replicates.

Replicate	Trans/Cis	PC%	PD%	IU/TU
Rep 1	1.187	25.8	74.2	3.88
Rep 2	1.196	23.2	76.8	4.00
Rep 3	1.246	28.9	71.1	3.75
Average	**1.209**	**26.0**	**74.0**	**3.88**
Std Dev	**0.032**	**2.8**	**2.8**	**0.12**

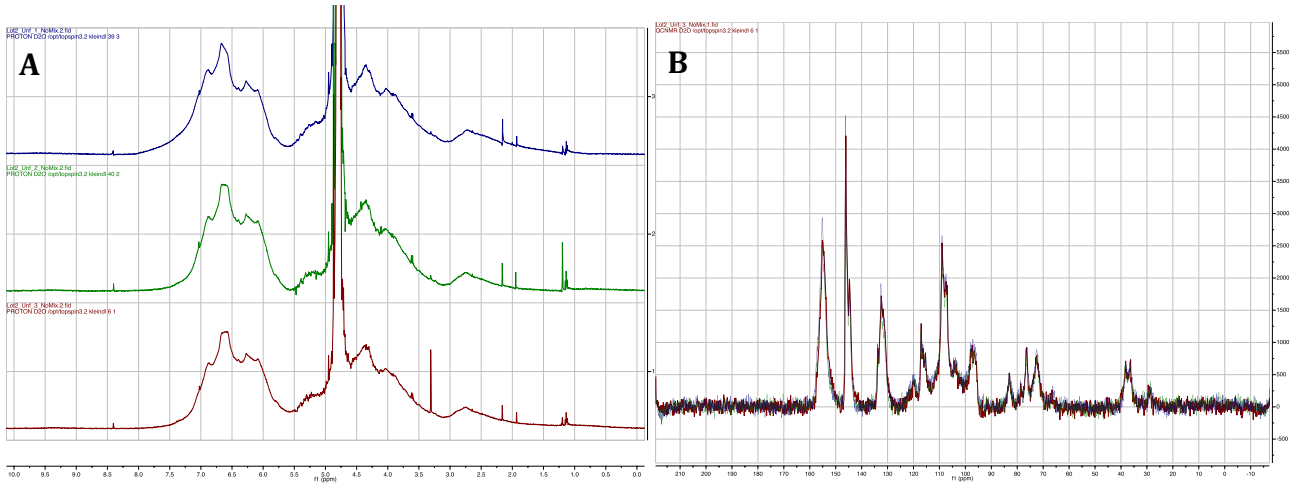

Figure 16: Triplicate spectra of Lot 2 (3117608). A) 1H NMR spectra. B) Overlaid qCNMR spectra.

Table 5: Calculated values of interest for Lot 2 (3117608) replicates.

Replicate	Trans/Cis	PC%	PD%	IU/TU
Rep 1	0.736	22.5	77.5	4.06
Rep 2	0.768	41.3	58.7	3.18
Rep 3	0.671	40.0	60.0	4.06
Average	**0.725**	**34.6**	**65.4**	**3.77**
Std Dev	**0.049**	**10.5**	**10.5**	**0.51**

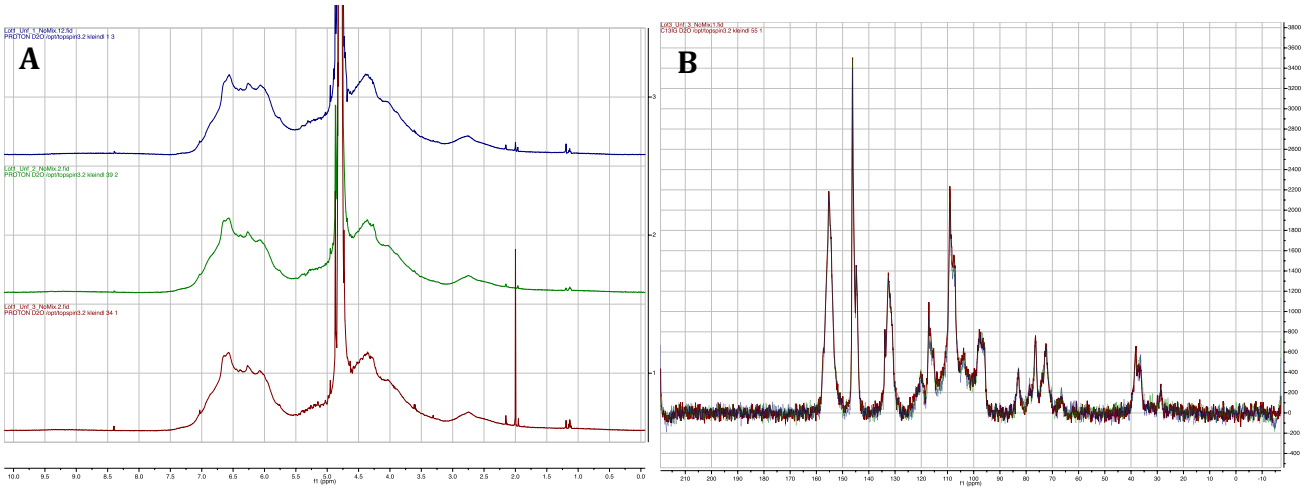

Figure 17: Triplicate spectra of Lot 3 (3125951). A) 1H NMR spectra. B) Overlaid qCNMR spectra.

Table 6: Calculated values of interest for Lot 3 (3125951) replicates.

Replicate	Trans/Cis	PC%	PD%	IU/TU
Rep 1	0.734	31.8	68.2	5.66
Rep 2	0.666	41.5	58.5	5.76
Rep 3	0.617	31.2	68.8	4.93
Average	**0.672**	**34.9**	**65.1**	**5.45**
Std Dev	**0.058**	**5.8**	**5.8**	**0.45**

Table 7: Summary of calculated values from qCNMR for each lot.

	Trans/Cis	PC%	PD%	IU/TU
Lot 1	1.209 ± 0.037	26.0 ± 5.8	74.0 ± 5.8	3.88 ± 0.14
Lot 2	0.725 ± 0.057	34.6 ± 12.2	65.4 ± 12.2	3.77 ± 0.59
Lot 3	0.672 ± 0.068	34.9 ± 3.3	65.1 ± 3.3	5.45 ± 0.52

Average ± 2*SE

4.4 Mixture Studies

Though data collection of the mixtures is still underway, subtle differences can be seen between the different mixtures. Newly tested samples of the isolated lots correlate well with those recorded previously for batch-to-batch variability assessment. Values for spectra collected so far (n=2 of 3) are summarized in Table 8.

Table 8: Summary of calculated values from qCNMR for isolated lots and mixtures of unfractionated crofelemer.

	Trans/Cis	PC%	PD%	IU/TU
Lot 1 (n=2)	1.235 ± 0.079	25.4 ± 3.5	74.6 ± 3.5	5.55 ± 0.27
Lot 2 (n=2)	0.740 ± 0.063	38.8 ± 1.1	61.2 ± 1.1	3.26 ± 0.22
Lot 3 (n=2)	0.678 ± 0.003	36.1 ± 1.3	63.9 ± 1.3	4.29 ± 0.44
Mix 1 (n=2)	0.813 ± 0.007	40.8 ± 3.8	59.2 ± 1.3	4.23 ± 0.07
Mix 2 (n=2)	0.696 ± 0.040	29.3 ± 1.2	70.7 ± 1.2	4.29 ± 0.31
Mix 3 (n=2)	0.987 ± 0.008	27.4 ± 3.3	72.6 ± 3.3	5.81 ± 0.22
Mix 4 (n=2)	0.723 ± 0.016	38.3 ± 3.9	61.7 ± 3.9	4.80 ± 0.44
Mix 5 (n=2)	0.694 ± 0.008	24.5 ± 3.8	75.5 ± 3.8	4.19 ± 0.30
Mix 6 (n=2)	0.693 ± 0.009	31.2 ± 5.8	68.8 ± 5.8	4.43 ± 0.14

5. Discussion

5.1 ^{1}H and Quantitative ^{13}C NMR of Forced Degradation Samples

Due to crofelemer's heterogeneity and polymeric nature, the peaks in the ^{1}H NMR spectra are considerably broad. The 2.0-3.1 ppm peak arises from the proton(s) located on the C4 sp3 hybridized carbon. The 3.1-5.5 ppm peak consists of the signals from the C2 and C3 sp3 hybridized carbons in their cis and trans conformations. The 5.5-7.3 ppm peak, perhaps the most distinctive peak in the ^{1}H NMR spectra, is composed of a collection of protons off of the sp2 hybridized carbons of the A and B rings of the repeating units. Broadening of any signature characteristics of the ^{1}H NMR peaks occurred over the course of sample incubation. It is hard to say whether the decrease in signal intensity results from simple concentration decreases due to precipitation of sample over time, a result of Hydrogen-Deuterium exchange, or representative of actual chemical degradations/changes occurring within the sample. That being said, significant changes in the 5.5-7.3 peak in particular could be indicative of further oxidation and/or PD to PC conversions that may be occurring over time.

The qCNMR spectra reveal more pertinent information about potential chemical and physical degradations that may occur in crofelemer over time. While some peak broadening did occur over the course of sample degradation, IU/TU, trans/cis ratios, and PC and PD percentages could be determined in most samples except for the 40ºC, 30 day unfractionated sample. When comparing time zero samples of unfractionated crofelemer to its MWCO fractions, a counter intuitive decrease in IU/TU ratios was observed. This could be contributed to retention of higher molecular weight fractions of crofelemer due to extensive hydrogen bonding with the polyphenol nature of the regenerated cellulose membrane used during sample preparations. Increases in the

IU/TU values of the 30 day, 40ºC fractionated samples compared to their time zero counterparts indicate potential chemical additions at the C4 position of terminal units.

The trans/cis ratios of each fraction and their respective degraded forms did not reveal any consistent trends. It is possible that the presence of regenerated cellulose altered signal contribution to the δ 76.6 ppm peak for cis moieties, however no consistent increase in cis composition was seen between unfractionated and MWCO fractions(Idström et al., 2016).

Increases in the presence of the procyanidin moieties, with consequent decreases in prodelphinidin moieties were observed across all fractions (excluding the 10 kDa Top, 30 day, 25ºC sample). The decrease in the 131-133 ppm signal range relative to total signal of the spectra indicates a loss of the triphenol structure of the gallocatechin units at the C5', C4' and C3' carbons. Interestingly an increase in the 146.2 ppm signal relative to total signal was observed. A simple conversion from gallocatechin to catechin units via loss of the C5' hydroxyl should not result in an increase of 146.2 signal, as catechin and gallocatechin moieties contribute equally to this peak.

5.2 T84 Chloride Channel Inhibition Assay

A fluorescent microplate assay was utilized for assessing total chloride efflux from T84 monolayers to assess variations of activity between crofelemer and its adulterated forms. Ideally, degradation of the starting material should result in observable changes in a drugs ability to initiate a measurable response. Though the exact mechanism of crofelemer in the GI tract is not known, it has been shown to selectively inhibit CaCC and CFTR chloride channels[(Tradtrantip et al., 2010)]. T84 cells express both CaCC and CFTR channels. By comparing total passive Cl- efflux (Blank) to efflux measured in the presence of crofelemer samples, the overall ability of

crofelemer to inhibit Cl- efflux could be quantified. Challenge of the crofelemer samples was performed using selective initiators of either CaCC (ionomycin) or CFTR (forskolin) in an effort to distinguish potential loss of inhibitive activity toward single channels after crofelemer degradation had occurred. Quercetin, a highly similar monomeric form of the catechin and gallocatechin subunits which comprise crofelemer, was used at higher concentrations (100 μM) in an effort to saturate Cl- channels as a positive control. The subtle changes from the initial lot of crofelemer during the degradation process did not have any substantial effect on its ability to inhibit Cl- efflux. Degradation of crofelemer did not substantially impact the polymers ability to inhibit individual channels when challenged with forskolin or ionomycin. It is entirely possible that the extent of degradation investigated in this study was not substantial for creating detectable changes in the chloride channel assay. As a heterogeneous polymeric species, slight or even substantial degradation in the repeating units of the overall chains that comprise the polymer may not cause observable changes in activity with the assay used. If only a single repeating unit and not a coherent chain of catechin and/or gallocatechin of crofelemer is necessary for chloride channel inhibition, then minor degradations in a sample of crofelemer – though observable through analytical analysis – may not translate into distinguishable changes in biological activities. This assumption could be further supported by quercetin's ability to inhibit chloride efflux as a single repeating unit mimic.

5.3 Initial Lot Variability Investigation and Mixture Studies

Quantitative ^{13}C NMR proved to be a data rich analytical tool when characterizing forced degradation samples of crofelemer. Unfortunately, due to limited sample availability and budget considerations, these degraded samples and their time zero counterparts were not tested in

triplicate. Because of this, the spectra could not be applied to initial model development using the machine learning approach. Regenerated cellulose contamination from the centrifugal filters used in the fractionation process also complicated top fraction analysis.

In initial lot variability measurements and in the mixture study, ^{1}H NMR and qCNMR spectra are being collected in triplicate to afford more statistical power to the data set. These spectra of the unfractionated lots and corresponding mixtures will be utilized in the mathematical modeling approach. While data collection of the final replicates is still underway, noticeable variation between different lots and the different mixtures can already be seen.

6. Conclusions

In this study, ^{1}H NMR and quantitative ^{13}C NMR was used to characterize various lots, degradants, and mixtures of crofelemer. A fluorescence microplate assay using T84 cell monolayers was also used to assess the inhibitive activity of unfractionated, fractionated, and degraded forms of a single lot of crofelemer on two chloride ion channels, CaCC and CFTR. Quantitative NMR proved to be a powerful analytical tool for observing changes in a crofelemer sample's average monomeric unit stereochemistry (trans/cis), number average molecular weight (IU/TU) and monomer compositions (PC and PD percentages). The T84 bioassay was unable to identify any significant differences between subtly degraded forms of crofelemer. Whether this is due to lack of sensitivity of the assay, lack of significant degradation to impact crofelemer activity, or degradations not specific or substantial enough to the structure(s) necessary for crofelemer activity is yet to be determined. After initial studies were performed on a single lot, the approach to NMR characterization was slightly modified to afford more statistical power and allow integration into mathematical model development and future crofelemer sample similarity assessment.

7. Future Work

The ultimate goal for the analysis of crofelemer and its degraded forms and mixtures is to combine this characterization data with other analytical techniques (UV-Vis, CD, FTIR, SEC, HILIC, RP-HPLC, and mass spectrometry). The entirety of the data set will then be used in a machine learning approach to develop a mathematical model capable of identifying assays or points of interest within assays (CQAs), which are most relevant to biological and clinical outcomes. The scope of this work will not encompass clinical data. Therefore correlation of CQAs identified by the models will be based on their ability to distinguish between subtle differences in samples tested. Improvements to the T84 bioassay are necessary to relate analytically observable differences in crofelemer samples to their ability to inhibit CaCC and CFTR. This optimization is currently underway, testing various concentrations of crofelemer tested and culture conditions used to reduce variability and improve sensitivity within the assay.

8. References

Canani, R. B., Cirillo, P., Mallardo, G., Buccigrossi, V., Secondo, A., Annunziato, L., . . . Guarino, A. (2003). Effects of HIV-1 Tat protein on ion secretion and on cell proliferation in human intestinal epithelial cells. *Gastroenterology, 124*(2), 368-376. doi:10.1053/gast.2003.50056

Chow, S. C., Song, F., & Bai, H. (2016). Analytical Similarity Assessment in Biosimilar Studies. *AAPS J, 18*(3), 670-677. doi:10.1208/s12248-016-9882-5

Davis, A. L., Cai, Y., Davies, A. P., & Lewis, J. R. (1996). 1H and 13C NMR assignments of some green tea polyphenols. *Magn Reson Chem, 34*, 887-890.

Diarrhoeal disease. (April 2013). Retrieved from http://www.who.int/mediacentre/factsheets/fs330/en/

Dong, Y., Zeng, C. Q.-Y., Ball, J. M., Estes, M. K., & Morris, A. P. (1997). The rotavirus enterotoxin NSP4 mobilizes intracellular calcium in human intestinal cells by stimulating phospholipase C-mediated inositol 1,4,5-triphosphate production. *Proc Natl Acad Sci U S A, 94*, 3960-3965.

Feasey, N. A., Healey, P., & Gordon, M. A. (2011). Review article: the aetiology, investigation and management of diarrhoea in the HIV-positive patient. *Aliment Pharmacol Ther, 34*(6), 587-603. doi:10.1111/j.1365-2036.2011.04781.x

Fischer, H., Machen, T. E., Widdicombe, J. H., Carlson, T. J., King, S. R., Chow, J. W., & Illek, B. (2004). A novel extract SB-300 from the stem bark latex of Croton lechleri inhibits CFTR-mediated chloride secretion in human colonic epithelial cells. *J Ethnopharmacol, 93*(2-3), 351-357. doi:10.1016/j.jep.2004.04.005

Gabriel, S. E., Davenport, S. E., Steagall, R. J., Vimal, V., Carlson, T., & Rozhon, E. J. (1999). A novel plant-derived inhibitor of cAMP-mediated fluid and chloride secretion. *Am J Physiol, 276*(Gastrointest Liver Physiol. 39), G58-G63.

Idström, A., Schantz, S., Sundberg, J., Chmelka, B. F., Gatenholm, P., & Nordstierna, L. (2016). 13C NMR assignments of regenerated cellulose from solid-state 2D NMR spectroscopy. *Carbohydrate Polymers, 151*, 480-487. doi:10.1016/j.carbpol.2016.05.107

Isogai, A. (1997). NMR analysis of cellulose dissolved in aqueous NaOH solutions. *Cellulose, 4*, 99-107.

Lorrot, M., & Vasseur, M. (2007). How do the rotavirus NSP4 and bacterial enterotoxins lead differently to diarrhea? *Virol J, 4*, 31. doi:10.1186/1743-422X-4-31

MacArthur, R. D., & DuPont, H. L. (2012). Etiology and pharmacologic management of noninfectious diarrhea in HIV-infected individuals in the highly active antiretroviral therapy era. *Clin Infect Dis, 55*(6), 860-867. doi:10.1093/cid/cis544

Maresca, M., Mahfoud, R., Garmy, N., Kotler, D. P., Fantini, J., & Clayton, F. (2003). The Virotoxin Model of HIV-1 Enteropathy: Involvement of GPR15/Bob and Galactosylceramide in the Cytopathic Effects Induced by HIV-1 gp120 in the HT-29-D4 Intestinal Cell Line. *Journal of Biomedical Science, 10*(1), 156-166. doi:10.1007/bf02256007

PMLiVE. (2016). Top 50 pharmaceutical products by global sales. Retrieved from http://www.pmlive.com/top_pharma_list/Top_50_pharmaceutical_products_by_global_sales

Rufo, P. A., Lin, P. W., Andrade, A., Jiang, L., Rameh, L., Flexner, C., . . . Lencer, W. I. (2004). Diarrhea-associated HIV-1 APIs potentiate muscarinic activation of Cl- secretion by T84

cells via prolongation of cytosolic Ca2+ signaling. *Am J Physiol Cell Physiol, 286*, C998-C1008.

Tradtrantip, L., Namkung, W., & Verkman, A. S. (2010). Crofelemer, an antisecretory antidiarrheal proanthocyanidin oligomer extracted from Croton lechleri, targets two distinct intestinal chloride channels. *Mol Pharmacol, 77*(1), 69-78. doi:10.1124/mol.109.061051

Ubillas, R., Jolad, S. D., Bruening, R. C., Kernan, M. R., King, S. R., Sesin, D. F., . . . Nakanishi, K. (1994). SP-303, an antiviral oligomeric proanthocyanidin from the latex of *Croton lechleri* (Sangre de Drago). *Phytomedicine, 1*, 77-106.

Van Arnum, P. (2013). Tracking growth in biologics. *Pharmaceutical Technology, 37*(2). Retrieved from http://www.pharmtech.com/print/197700?page=full

West, M. R., & Molloy, C. R. (1996). A microplate assay measuring chloride ion channel activity. *Anal Biochem, 241*, 51-58.

Yeo, Q. M., Crutchley, R., Cottreau, J., Tucker, A., & Garey, K. W. (2013). Crofelemer, a novel antisecretory agent approved for the treatment of HIV-associated diarrhea. *Drugs of Today, 49*(4), 239-252.

Zingmond, D. S., Kilbourne, A. M., Justice, A. C., Wenger, N. S., Rodriguez-Barradas, M., Rabeneck, L., . . . Bozzette, S. A. (2003). Differences in symptom expression in older HIV-positive patients: The veterans aging cohort 3 site study and HIV cost and service utilization study experience. *J Acquir Immune Defic Syndr, 33*(Suppl 2), S84-S92.